

# Dynamics of Disorder-Order Transitions in Hard Sphere Colloidal Dispersions in $\mu$ g

J.X. Zhu, M. Li, S.E. Phan, W. B. Russel, P.M. Chaikin, Princeton  
R. Rogers, W. Meyers, NASA Lewis  
Crew of Shuttle Columbia, STS-73

366-29  
8:00:00 68

## Abstract

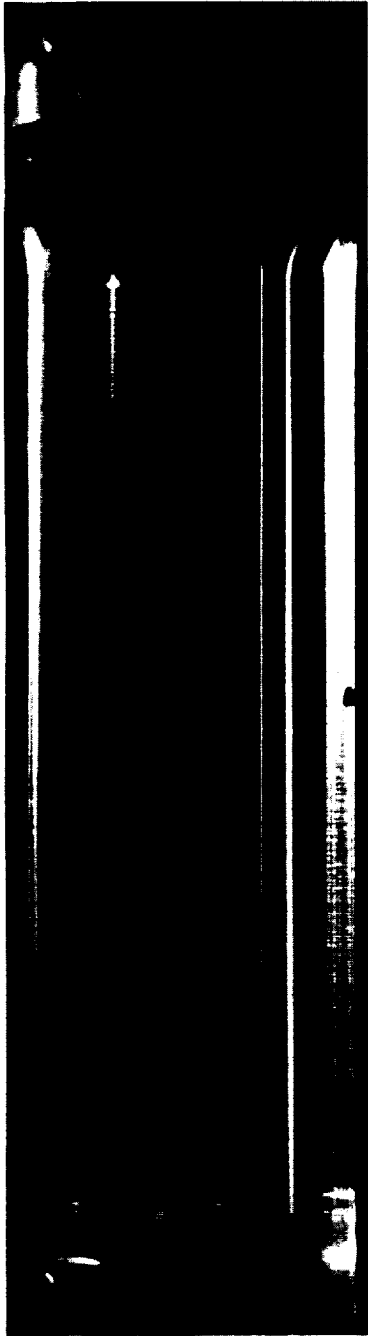
We have performed a series of experiments on  $0.518\mu\text{m}$  PMMA spheres suspended in an index matching mixture of decalin and tetralin in the microgravity environment provided by the Shuttle Columbia on mission STS-73. The samples ranged in concentration from 0.49 to 0.62 volume fraction ( $\phi$ ) of spheres, which covers the range in which liquid, coexistence, solid and glass phases are expected from earth bound experiments. Light scattering was used to probe the static structure, and the particle dynamics. Digital and 35mm photos provided information on the morphology of the crystals. In general the crystallites grew considerably larger (roughly an order of magnitude larger) than the same samples with identical treatment in one g. The dynamic light scattering shows the typical short time diffusion and long time caging effects found in one g. The surprises that were encountered in  $\mu$ g include the preponderance of RHCP (Random Hexagonal Close Packed) structures and the complete absence of the expected Face Centered Cubic (FCC) structure, existence of large dendritic crystals floating in the coexistence samples (where liquid and solid phases coexist) and the rapid crystallization of samples which exist only in glass phase under the influence of one g. These results suggest that colloidal crystal growth is profoundly effected by gravity in yet unrecognized ways. We suspect that the RCHP structure is related to the nonequilibrium growth that is evident from the presence of dendrites. An analysis of the dendritic growth instabilities is presented within the framework of the Ackerson - Schatzel equations.

## Introduction

The CDOT (Colloidal Disorder-Order Transition) experiment consisted of two parts, 1) photographic investigation of the phase diagram (liquid, crystal, glassy regimes) and crystallite morphology and 2) light scattering and shear modulus measurements of the monodispersed samples in the CDOT hardware operated in the shuttle glovebox. A detailed description of the CDOT hardware is to be found elsewhere in this conference. The samples were mixed each day prior to liftoff to prevent sedimentation. A day after orbit was achieved the samples were unstored and mixed in  $\mu$ g. Photographs and further experiments were performed after the samples had been in  $\mu$ g for three or more days after the  $\mu$ g mix. The mix was performed using a magnetic stirbar drawn through the sample in a prearranged series of translations and rotations and the samples were visually inspected by the astronauts after mixing to assure homogeneity and the absence of any remnant crystals.

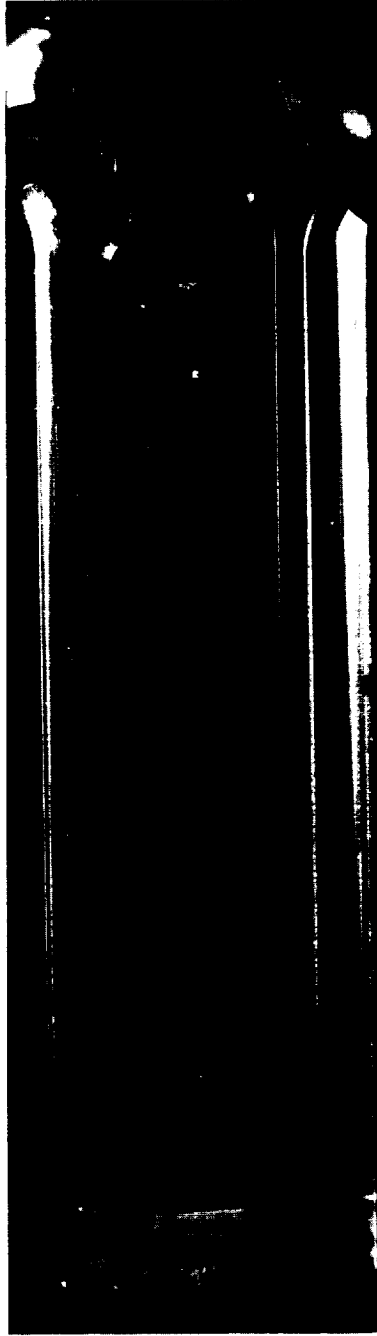
## Dendritic growth

Figure 1 shows photos of a sample in the coexistence region with volume fraction  $\phi=0.52$ . The left photo is taken on earth and shows liquid solid phase separation in gravity with the denser crystalline phase occupying the lower half of the tube and liquid in the upper half. In  $\mu$ g the crystallites remain suspended in the liquid phase. In addition to the larger crystallite size, an enlargement of part of the photo shows the existence of branched or dendritic crystals with dimensions  $\sim 2$  mm and characteristic structure on the scale  $100\mu$ . Although there have been hints of dendritic growth observed during nucleation experiments[1], and for soft potentials on a lower surface[2], this is the first clear evidence that the dominant growth mode of the hard sphere colloid is dendritic. In the following section we study why this phenomena is related to  $\mu$ g and whether the crystalline growth is intrinsically unstable.



**▲On Earth**

Gravity-driven sedimentation produces a volume fraction gradient from top to bottom. The liquid phase at the top appears transparent while crystallites can be observed in the lower portion of the cell.



**◀ In Microgravity**

In the low gravity environment of space, the spheres remain evenly dispersed in the cell and large crystallites formed in many of the samples. The shapes of many of these large crystallites indicate dendritic growth.

In comparing the effects of gravity to thermal processes, whether equilibrium or kinetic, a relevant quantity is the gravitational length,  $h = kT/mg$  ( $\sim 6\mu$  or 12 particle diameters for our particles), the height over which thermal energy can support a particle. Now consider nucleation and growth in the presence of gravity. If the solid phase is energetically favored then fluctuations can produce a crystallite in the liquid phase which will grow if it is larger than the critical nucleation radius. The crystalline droplet has a higher density than the surrounding fluid and will begin to sediment. The Stokes drag on the crystallite produces a stress proportional to the weight and inversely proportional to the cross section. When this stress exceeds the yield stress  $\sigma_{crit}$  of the crystallite, then the surface (and particularly any dendrites) will be sheared off. The condition can be written as  $\frac{\Delta M g}{4\pi R^2} = \sigma_{crit} \sim G \sim \frac{\alpha kT}{a^3}$ ,  $\Delta M = \frac{4}{3}\pi R^3 \Delta\phi \Delta\rho$ , where  $\Delta\phi$  is the density difference between PMMA and the solvent,  $\Delta\phi$  is the volume fraction difference between liquid and solid in coexistence,  $\alpha$  is a constant of order unity,  $G$  is the shear modulus and the yield stress is taken in its limiting form relative to  $G$ . The upper limit for the size of freely sedimenting crystals is then:

$$R_{crit} = \frac{\alpha kT}{\frac{4}{3}\pi a^3 g \Delta\phi \Delta\rho} = \frac{h}{\Delta\phi} \sim 20h$$

which amounts to about  $100\mu$  for our samples.

A more severe limitation on the observation of dendritic growth relates to whether the particle flux around the sedimenting crystallite is determined by convection or diffusion. This ratio is the Peclet number which for a single particle is simply the ratio of the particle radius to the gravitational length:

$$Pe_0 = \frac{vl}{D} = \frac{\left(\frac{\Delta\rho g \frac{4}{3}\pi a^3}{6\pi\eta a}\right)a}{kT/6\pi\eta a} = \frac{mga}{kT} = \frac{a}{h}$$

for a falling crystallite of dimension  $R$  the Peclet number becomes:

$$Pe_{cryst} = \frac{\left(\frac{(\Delta\rho g \frac{4}{3}\pi R^3)\Delta\phi}{6\pi\eta R}\right)R}{kT/6\pi\eta R} = \frac{a}{h} \frac{R^4}{a^4} \Delta\phi = Pe_0 \Delta\phi \frac{R^4}{a^4}$$

thus in order to observe dendritic growth at one  $g$  we would be limited to growth below

$$Pe_{cryst} \sim 1 \Rightarrow R_{crit} = a \left(\sqrt[4]{\frac{h}{a\Delta\phi}}\right) \sim 5a$$

We would expect dendrites to anneal from both self and gradient diffusion processes. The characteristic times for these processes vary as  $\frac{1}{\tau} \propto \frac{D_s}{R^2}$  and  $\frac{1}{\tau} \propto \frac{\gamma}{\eta R}$  where  $D_s$  is the self diffusion constant and  $\gamma$  is the surface tension. For our parameters self diffusion dominates and leaves structures of dimensions  $100\mu$  rough (unannealed) after three days.

Ackerson and Schatzel Growth Model

In order to model their pioneering experiments of the growth of hard sphere colloidal crystals Ackerson and Schatzel[3] wrote down the following equations governing the growth of the interface separating solid and liquid regions and solved them numerically for a spherical droplet.

$$\begin{aligned} \Pi_s(\phi_s) &= \Pi_f(\phi_f) + \frac{2\gamma}{R} && \text{pressure balance} \\ \frac{dR}{dt} &= \alpha \left[ \frac{D_s(\phi_f)}{2a} \right] \left[ 1 - \exp\left(\frac{(\mu_f(\phi_f) - \mu_s(\phi_s))}{kT}\right) \right] && \text{growth kinetics} \\ \frac{dR}{dt} (\phi_s - \phi_f) &= n \cdot [D_c^f \nabla \phi_f - D_c^s \nabla \phi_s] && \text{flux balance} \end{aligned}$$

Briefly, the first equation equates the osmotic pressure inside the droplet to the exterior pressure plus the Laplace pressure generated by the curvature  $1/R$ , and the surface tension  $\gamma$ . The second term weights the rate at which particles collide with the surface by the sticking probability. The third term says that the additional particle density accumulating at the growing interface is supplied by the net particle diffusion to the interface from the neighboring fluid and solid regions. These equations are then combined with the continuity equations in the solid and fluid phases.

$$\frac{\partial \varphi_s}{\partial t} = \nabla \cdot (D_c'(\varphi_s) \nabla \varphi_s) \quad \frac{\partial \varphi_f}{\partial t} = \nabla \cdot (D_c'(\varphi_f) \nabla \varphi_f)$$

These equations bear resemblance to the equations often used in the study of the dendritic instability:  $\frac{dR}{dt}(\varphi_s - \varphi_f) = n \cdot [D_c' \nabla \varphi_f - D_c' \nabla \varphi_s]$  and  $\mu - \mu_{equil} = -\frac{\gamma}{\Delta C} \kappa$  where  $\kappa$  is the local curvature. The second equation is the Gibbs-Thomson relation which is an approximation to the actual pressure discontinuity and the actual chemical potential equality for equilibrium. The growth kinetics are absent in this model under the assumption that the kinetic coefficient is so large the growth rate is self consistently limited by the Gibbs-Thomson relation which controls the the growth exponential.

With dimensionless definitions for kinetic coefficient,  $\delta = \frac{ID_s^0}{2aD_0}$ , critical radius,  $l = \frac{8\pi\gamma a^3}{3\varphi_s(\mu_f - \mu_s)}$ , chemical

potential,  $\mu = \mu/kT$ , and surface tension  $K = \gamma a^3/kT$  and with cooperative diffusion at high volume fraction approximately equal to the Stokes-Einstein diffusion constant we have the dimensionless growth equations as:

$$\begin{aligned} \Pi_s &= \Pi_f + 2\kappa K \\ \frac{dX}{dt} &= \delta [1 - e^{\Delta\mu}] \\ \frac{dX}{dt} &= \frac{n \cdot [D_c' \nabla \varphi_f - D_c' \nabla \varphi_s]}{(\varphi_s - \varphi_f)} \end{aligned}$$

The nature of the growth process depends only on the initial volume fraction  $\phi_0$  and particularly on the depth to which the sample is quenched into the solid phase as characterized by the undercooling parameter  $\Delta = \frac{\varphi_0 - \varphi_{freeze}}{\varphi_{melt} - \varphi_{freeze}}$ . Here  $\varphi_{freeze}$

is the lowest volume fraction at which hard spheres start to form crystals from the liquid ( $\varphi_{freeze}=0.49$ ) and  $\varphi_{melt}$  is the highest volume fraction at which the crystal phase begins to melt ( $\varphi_{melt}=0.54$ ). Physically the "quench" is accomplished by forcing the sample into the fluid state by vigorous shear melting. Generally we follow the spirit of the treatments of Ackerson and Schatzel[3] and Langer[4]. With the dimensionless growth equations and the boundary conditions:

$$\varphi_s(0, \tau) = const, \quad \varphi_f(\infty, \tau) = \varphi_0, \quad \varphi_f(\rho, 0) = \varphi_0, \rho > 1$$

there are pseudo-steady solutions corresponding to rapid growth for large undercooling ( $\Delta \gg 1$ , a quench deep into the solid regime) and slow growth (for  $\Delta \ll 1$ , in the coexistence region near the fluid phase).

The profile for rapid growth is described by:

$$\varphi_s = \varphi_{si} = \varphi_0, \quad \varphi_f = \varphi_0 - (\varphi_0 - \varphi_f) e^{-\frac{dX}{dt}(\rho-x)}, \quad \frac{dX}{dt}(\varphi_{si} - \varphi_f) = \nabla \varphi_f - \nabla \varphi_s = \frac{dX}{dt}(\varphi_0 - \varphi_f)$$

and is illustrated in figure 2 left. The equation and profile are the same as for a plane interface.

The profile for slow growth is described by:

$$\varphi_f = \varphi_0 - (\varphi_{freeze} - \varphi_{f0}) \frac{X}{\rho}, \quad X^2 = 2\Delta t$$

$$\frac{dX}{dt}(\varphi_{melt} - \varphi_{freeze}) = \nabla \varphi_f = \frac{-X}{\rho^2}(\varphi_{freeze} - \varphi_0) = \frac{(\varphi_0 - \varphi_{freeze})}{X}$$

$$\frac{XdX}{dt} = \frac{\varphi_0 - \varphi_{freeze}}{\varphi_{melt} - \varphi_{freeze}} = \Delta$$

and is illustrated in figure 2 right.

### Rapid Growth

### Slow Growth

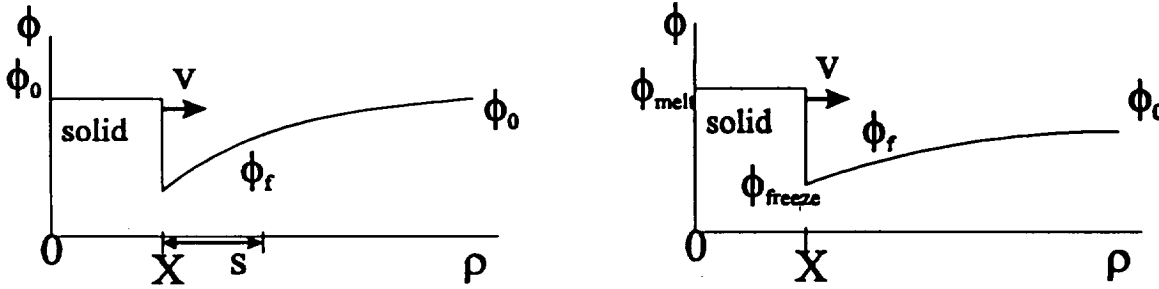


Fig. 2 Volume fraction (concentration) profiles for the pseudo steady solutions to the spherical growth model of references[3] and [5]. Left for rapid growth (strong undercooling). Right for slow growth.

These solutions describe the growth of spherical crystallites. We wish to see whether they are linearly stable to a perturbation which distorts the surface as a spherical harmonic.

The surface is taken as:  $\rho = x + \varepsilon Y_{jm}(\Theta, \Phi)e^{\omega_j t}$ . The volume fraction is perturbed with a similar symmetry and a coefficient  $\phi_j^1$  for which we must self consistently solve.

$$\varphi = \varphi^0(\rho, \tau) + \varepsilon \phi_j^1(\rho, \tau) Y_{jm}(\Theta, \Phi) e^{\omega_j t} \text{ the curvature is } \nabla^2 Y_{jm} = -\frac{j(j+1)Y_{jm}}{X^2}$$

or "rapid growth" the rate at which the perturbation develops,  $\omega_j$ , is given

$$\text{by: } \omega_j = \frac{j}{X} \dot{X} \left\{ 1 - \frac{K}{\Delta \varphi \Pi_j \dot{X}} \frac{j^2}{X^2} \frac{\pi_j / \varphi_j + \pi_j / \varphi_s}{\pi_j / \varphi_j - \pi_j / \varphi_s} \right\} \text{ or } \omega_j = kv \frac{l^2}{D_0} \left\{ 1 - (1 + \beta) k^2 \frac{D_0 \gamma}{v(\Delta C)^2 (\partial \mu / \partial c)} \right\} \text{ with } kl = j/X$$

which is the same form in detail as the Mullins-Sekerka instability. Likewise for "slow growth" the perturbation develops

$$\text{with rate: } \omega_j = \frac{(j-1)}{X} \dot{X} \left\{ 1 - \frac{(J+2) K}{\Delta \varphi \Pi_j \dot{X}} \frac{\pi_j / \varphi_j + (j+1)\pi_j / \varphi_s}{\pi_j / \varphi_j - \pi_j / \varphi_s} \right\} \text{ or}$$

$$\omega_j = (j-1) \frac{v}{R} \left\{ 1 - \frac{((1+\beta)j+1)(j+2)}{R^2} \frac{D_0 \gamma}{v(\Delta C)^2 (\partial \mu / \partial c)} \right\} \text{ with } v = \dot{X} \frac{D_0}{l} \text{ and } \beta = \frac{\pi_j / \varphi_j}{\pi_j / \varphi_s} \text{ which is the same as for the}$$

simpler growth model and is unstable when the crystallite grows to more than about 7 critical radii or about  $49a \sim 13\mu$  for our samples.

These results indicate that the spherical growth is linearly unstable to the formation of a modulated surface early in the growth. Presumably these modulations will develop into the dendritic arms which we observe. However, as in most cases of dendritic growth, the characteristic size of the dendrites is determined by the growth velocity which depends itself on the

finger width typically as:  $v_R = \frac{D}{R} \left( \Delta - \frac{2d_0}{R} \right)$ . The equations allow for a variety of velocities and tip radii. If we take the

Glickman result that  $v \sim v_{\max}/50$  and use the number shown in table 1 we find that the dendrite size is  $\lambda \sim 140\mu$  as in our CDOT experiment.

Table 1. definitions and values for lengths used in the dendritic growth calculations

|                  | Definition  | value at $\phi=0.52$<br>a=particle radius |
|------------------|---|---|
| critical nucleus | $\frac{\Gamma^*}{a} = \frac{8\pi\gamma a^2}{3\phi_s(\mu_f - \mu_s)}$                            | $\sim 7a$                                 |
| capillary length | $d_0 = \frac{\gamma}{(\Delta C)^2 \left(\frac{\partial \mu}{\partial C}\right)}$                | $\sim 2a$                                 |
| diffusion length | $l = \frac{2D}{v} \sim \frac{2D_c(\phi)}{\left(D_s(\phi)/2a\right) \left(1 - e^{-w/kr}\right)}$ | $> 80a$                                   |
| dendrite size    | $\lambda = 2\pi\alpha\sqrt{ld_0}$   | $\sim 80a \quad \sim 20\mu$               |

### Conclusions

In this paper we have addressed a few of the aspects of the CDOT experiment concentrating on the dendritic growth. We also observed that all of the samples which were supposed to be in the glassy state, and never crystallized on the ground, did form crystals in orbit. The static light scattering exhibited very strong narrow "streaks" indicating large crystallites with a RHCP structure and none of the FCC observed on ground. The absence of a glass phase or an FCC phase are unexpected effects of  $\mu g$  which deserve further attention and point to some very subtle effects of gravity on crystal nucleation and growth.

Research supported by NASA under grant NAG3-1762.

### References

- [1] K. Schatzel and B. J. Ackerson, Phys. Rev. Lett. **68**, 337 (1992).
- [2] A. P. Gast and Y. Monovoukas, Nature, **351**, 553 (1991).
- [3] B. J. Ackerson and K. Schatzel, Phys. Rev. **B52**, (1995).
- [4] J. S. Langer, Rev. Mod. Phys. **52**, 1 (1980).
- [5] W. B. Russel et al., to be published.